Optimal Charging of Batteries via a Single Particle Model with Electrolyte and Thermal Dynamics

H. E. Perez, X. Hu, and S. J. Moura

***Abstract*— This paper seeks to derive insight on battery charging control using electrochemistry models. Directly using full order complex multi-partial differential equation (PDE) electrochemical battery models is difficult and sometimes impossible to implement. This paper develops an approach for obtaining optimal charge control schemes, while ensuring safety through constraint satisfaction. An optimal charge control problem is mathematically formulated via a coupled reduced order electrochemical-thermal model which conserves key electrochemical and thermal state information. The Legendre-Gauss-Radau (LGR) pseudo-spectral method with adaptive multi-mesh-interval collocation is employed to solve the resulting nonlinear multi-state optimal control problem. Minimum time charge protocols are analyzed in detail subject to solid and electrolyte phase concentration constraints, as well as temperature constraints. The optimization scheme is examined using different input current bounds, and an insight on battery design for fast charging is provided.**

I. Introduction

This paper develops an approach to solve for optimal charge control schemes using an electrochemical based model with thermal dynamics. The goal is to systematically obtain optimal charge schemes that result in the lowest charge times, while understanding their nature to gain an insight on battery design optimization for fast charging.

Batteries are widely utilized in mobile handsets, electric vehicles (EVs), and power grid energy storage [1], [2]. They are an enabling technology for diversifying and securing our future energy supplies. In contrast to simple and rapid refueling of gasoline or diesel, battery recharge requires meticulous control and management, owing to complex electrochemical reactions, immeasurable internal states, and serious safety concerns [3]. Fast charging is a thriving area of research, as it increases the practicality and consumer acceptance of battery-powered devices (e.g., EVs). Nevertheless, it can also impair battery longevity depending on the charging method used, particularly due to heating. It is thus crucial to systematically study the effects of electrochemical states on charging time, which is the focus of this paper.

The traditional charging protocol for Li-ion batteries is constant-current/constant-voltage (CC-CV) [4]. In the CC stage, the charging current is constant until a pre-specified voltage threshold is reached, and in the CV stage the voltage threshold is maintained until the current relaxes below a pre-specified threshold value. This technique is simple and easily implemented. The current rate and voltage threshold are, however, almost universally selected in an ad-hoc manner.

H. E. Perez, X. Hu, and S. J. Moura are with Civil and Environmental Engineering, University of California, Berkeley, CA 94720, USA E-mail: {heperez, xiaosonghu, smoura}@berkeley.edu

In the literature, various methods have been proposed to reduce charge times, such as multi-stage CC (high CC followed by low CC) plus CV (CC-CC-CV) [5], boost charging (CV-CC-CV) [6], constant power-constant voltage (CP-CV) [7], fuzzy logic [8], [9], neural networks [10], grey system theory [11], and ant colony system algorithm [12]. Alternative protocols were reported to prolong the battery lifetime as well, such as MCC-CV (low CC followed by high CC plus CV) [7] and CC-CV with negative pulse (CC-CV-NP) [13]. This literature provides enormous insight on rapid charging, but all the protocols are – at some level – heuristic. That is, they employ basic knowledge, empirical observations, and experience of the battery's electrical properties to devise a charging strategy. Their implementation and performance are subject to cumbersome meta-parameter tuning. Furthermore, there are no mathematical guarantees for fast charge optimality, nor constraint satisfaction.

Recently, some researchers have given first insights into model-based optimal charge control [14], [15], [16], [17], [18], [19]. A significant challenge for model-based charge control is numerically solving a multi-state nonlinear calculus of variations optimal control problem. These previous studies side-step this difficulty using linear-quadratic formulations [14], state independent electrical parameters [15], piecewise constant time discretization [16], linear input-output models [17], a one-step model predictive control formulation [18], or a reference governor formulation [19]. To directly face the nonlinear variational calculus problem, orthogonal collocation enabled pseudo-spectral methods were employed in [20] to optimize charging time and efficiency of lithium-ion batteries. This work was extended in [21] to consider aging and coupled electrical-thermal dynamics via equivalent circuit type models. However, all of the foregoing studies do not explore coupled electrochemical and thermal dynamics for fast charge applications. Moreover, previous model based techniques do not give insight on what parameters a battery cell designer can optimize for enabling faster charge times.

This paper pursues a different approach to developing optimal fast charging protocols using electrochemical-thermal models. Mathematically, we formulate a minimum time optimal control problem via a coupled Single Particle Model with Electrolyte and Thermal Dynamics (SPMeT). In the coupled model, two PDE single particle subsystems capture both anode and cathode solid concentration dynamics, a three-PDE electrolyte subsystem captures the electrolyte concentration dynamics in three domains (anode, separator, cathode) which all feed into the nonlinear voltage output function (10). The

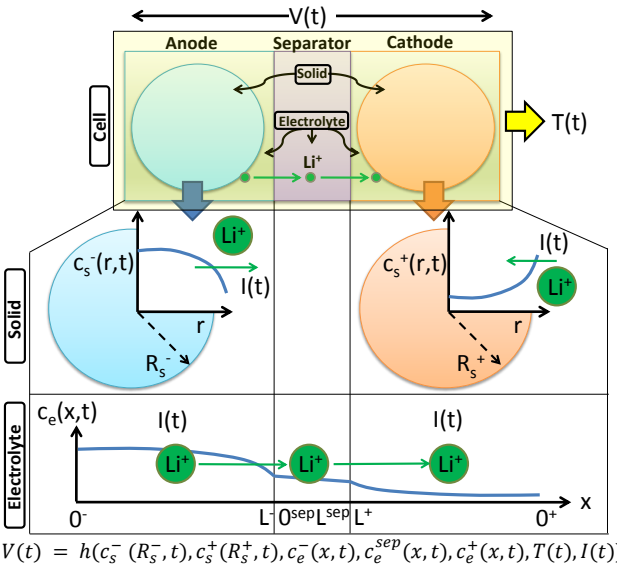

Fig. 1. Each electrode is idealized as a single porous spherical particle whose dynamics evolve in the r dimension. The electrolyte concentration dynamics evolve in all regions in the x dimension.

nonlinear voltage output and bulk solid concentrations are then fed into the thermal subsystem (12), whose temperature feeds back into the nonlinear voltage output. Due to the coupled electrochemical-thermal dynamics, the optimization problem is highly nonlinear. Consequently, there are no analytic solutions and numerical solutions have been considered extremely difficult. We challenge this entrenched mindset by leveraging the Legendre-Gauss-Radau (LGR) pseudo-spectral method with adaptive multi-mesh-interval collocation.

The remainder of this paper is structured as follows. In Section II, the Single Particle Model with Electrolyte and Thermal Dynamics is described. In Section III, the minimum time optimal charge control problem is formulated, and the LGR pseudo-spectral method is briefly introduced. Optimization results are discussed in Section IV, followed by conclusions in Section V.

II. Single Particle Model with Electrolyte and Thermal Dynamics

The Single Particle Model with Electrolyte and Thermal Dynamics (SPMeT) is summarized in this section. The Single Particle Model with Electrolyte Dynamics (SPMe) used here is most similar to [22], [23], [24] and achieves a higher prediction accuracy than the Single Particle Model without electrolyte dynamics. Complete details on the derivation and model properties of the SPMe are presented in [25]. The Thermal Model from [26] is coupled to the SPMe to form the SPMeT (see Fig. 1).

A. SPMeT Model

The SPMeT model consists of: (i) two linear spherical diffusion PDEs modeling each electrode's solid concentration dynamics, (ii) a quasilinear diffusion equation (across three domains) modeling the electrolyte concentration dynamics, (iii) a nonlinear output function mapping boundary values

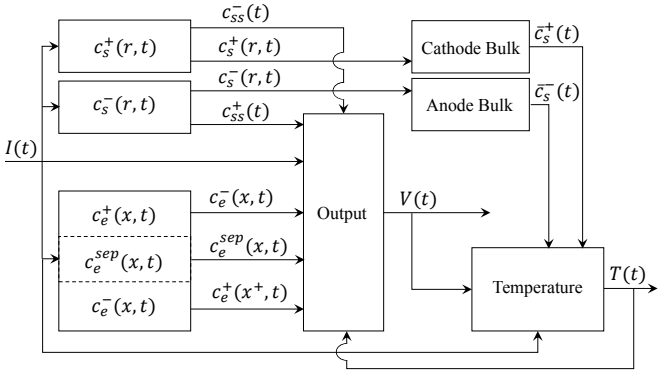

Fig. 2. Block diagram of SPMeT. Note that the c_s^+, c_s^-, c_e subsystems are independent of one another, and that temperature feeds back into the nonlinear voltage output.

of solid concentration, electrolyte concentration, and current to terminal voltage, and (iv) a nonlinear ODE modeling the bulk temperature of the cell which then feeds back into the nonlinear output function (see Fig. 2).

We now introduce the SPMeT equations. The solid diffusion equations (1) with boundary conditions (2) are

$$\frac{\partial c_s^\pm}{\partial t}(r,t) = \frac{1}{r^2}\frac{\partial}{\partial r}\left[D_s^\pm r^2 \frac{\partial c_s^\pm}{\partial r}(r,t)\right], \tag{1}$$

$$\frac{\partial c_s^\pm}{\partial r}(0,t) = 0, \quad \frac{\partial c_s^\pm}{\partial r}(R_s^\pm,t) = \mp\frac{1}{D_s^\pm F a^\pm L^\pm} I(t). \tag{2}$$

The Neumann boundary conditions at $r = R_s^\pm$ signify the flux entering the electrode is proportional to the input current $I(t)$ (positive for charge). The Neumann boundary conditions at $r = 0$ are spherical symmetry conditions and required for well-posedness. Next, the electrolyte diffusion equations (3)-(5) with boundary conditions (6)-(9) are

$$\frac{\partial c_e^-}{\partial t}(x,t) = \frac{\partial}{\partial x}\left[D_e(c_e^-)\frac{\partial c_e^-}{\partial x}(x,t)\right] - \frac{(1-t_c^0)}{\varepsilon_e^- F L^-} I(t), \tag{3}$$

$$\frac{\partial c_e^{\text{sep}}}{\partial t}(x,t) = \frac{\partial}{\partial x}\left[D_e(c_e^{\text{sep}})\frac{\partial c_e^{\text{sep}}}{\partial x}(x,t)\right], \tag{4}$$

$$\frac{\partial c_e^+}{\partial t}(x,t) = \frac{\partial}{\partial x}\left[D_e(c_e^+)\frac{\partial c_e^+}{\partial x}(x,t)\right] + \frac{(1-t_c^0)}{\varepsilon_e^+ F L^+} I(t), \tag{5}$$

$$\frac{\partial c_e^-}{\partial x}(0^-,t) = \frac{\partial c_e^+}{\partial x}(0^+,t) = 0, \tag{6}$$

$$\varepsilon_e^- D_e(L^-)\frac{\partial c_e^-}{\partial x}(L^-,t) = \varepsilon_e^{\text{sep}} D_e(0^{\text{sep}})\frac{\partial c_e^{\text{sep}}}{\partial x}(0^{\text{sep}},t), \tag{7}$$

$$\varepsilon_e^{\text{sep}} D_e(L^{\text{sep}})\frac{\partial c_e^{\text{sep}}}{\partial x}(L^{\text{sep}},t) = \varepsilon_e^+ D_e(L^+)\frac{\partial c_e^+}{\partial x}(L^+,t), \tag{8}$$

$$c_e(L^-,t) = c_e(0^{\text{sep}},t), \quad c_e(L^{\text{sep}},t) = c_e(L^+,t). \tag{9}$$

The nonlinear output function for terminal voltage is governed by a combination of electric overpotential, electrode thermodynamics, Butler-Volmer kinetics, and electrolyte potential as

$$V(t) = \frac{RT(t)}{\alpha F}\sinh^{-1}\left(\frac{I(t)}{2a^+L^+\bar{i}_0^+(t)}\right)$$

$$
\begin{aligned}
&- \frac{RT(t)}{\alpha F} \sinh^{-1}\left(\frac{-I(t)}{2a^- L^- \bar{i}_0^-(t)}\right) \\
&+ U^+(c_{ss}^+(t)) - U^-(c_{ss}^-(t)) \\
&+ \left(\frac{R_f^+}{a^+ L^+} + \frac{R_f^-}{a^- L^-}\right) I(t) - \frac{L^+ + 2L^{\text{sep}} + L^-}{2\overline{\kappa}} I(t) \\
&+ k_{\text{conc}}(t)\left[\ln c_e(0^+,t) - \ln c_e(0^-,t)\right], \qquad (10)
\end{aligned}
$$

where $c_{ss}^{\pm}(t) = c_s^{\pm}(R_s^{\pm},t)$ is the surface concentration in the solid, $k_{\text{conc}} = \frac{2RT(t)}{F}(1-t_c^0)\bar{k}_f(t)$, and $\bar{i}_0^{\pm}(t)$ is the spatially averaged exchange current density

$$
i_0^{\pm}(t) = k^{\pm}\left[c_{ss}^{\pm}(t)\right]^{\alpha_c}\left[c_e^{\pm}(x,t)\left(c_{s,\max}^{\pm} - c_{ss}^{\pm}(t)\right)\right]^{\alpha_a}. \qquad (11)
$$

The bulk temperature dynamics which includes ambient, ohmic and entropic heating terms is governed by

$$
\begin{aligned}
\frac{dT(t)}{dt} &= \frac{h_{cell}}{\rho^{avg} c_p}(T_{amb}(t) - T(t)) \\
&+ \frac{I(t)}{\rho^{avg} c_p}\left[V(t) - (U^+(\bar{c}_s^+(t)) - U^-(\bar{c}_s^-(t)))\right] \\
&+ \frac{I(t)T(t)}{\rho^{avg} c_p} \cdot \frac{\partial}{\partial T}\left[U^+(\bar{c}_s^+(t)) - U^-(\bar{c}_s^-(t))\right] \qquad (12)
\end{aligned}
$$

where $\bar{c}_s^{\pm}(t)$ is the bulk concentration in the anode/cathode

$$
\bar{c}_s^{\pm}(t) = \frac{3}{(R_s^{\pm})^3}\int_0^{R_s^{\pm}} r^2 c_s^{\pm}(r,t)dr. \qquad (13)
$$

We define bulk anode SOC as

$$
SOC(t) = \frac{\bar{c}_s^-(t)}{c_{s,max}^-}. \qquad (14)
$$

This summarizes the SPMeT which maintains accuracy at higher C-rates than that of an SPM with thermal dynamics alone [25]. The model parameters used in this study originate from the publicly available DUALFOIL simulation package [27] and correspond to a lithium cobalt oxide cathode / graphite anode chemistry. The cell capacity is 40.18 Ah/m^2, calculated from the maximum concentration of the anode.

1) Comparison to existing SPMe Models: The models in [22], [23], [24] are most similar to the SPMe presented here with a few critical differences. In [22], bulk solid concentration is used in the voltage output function instead of the surface concentration we use here (see (26) in [22]). In the case of [23], volume averaging is performed in the electrolyte phase which partially obscures electrolyte polarization. In [24], the authors use an approximation of the solid state diffusion equation instead of retaining the PDE version we use in (1)-(2) (see Section 2 of [24]). Moreover, we include a temperature submodel, as does [22].

III. Optimal Charge Control Formulation

Next we formulate a minimum-time/safe optimal charge control problem. The objective function J is given by

$$
\min_{I(t),x(t),t_f} \int_{t_0}^{t_f} 1 \cdot dt, \qquad (15)
$$

where $(t_f - t_0)$ is the charge time to reach a desired target SOC (SOC_f). The optimization variables are the input current $I(t)$ and final time t_f, with state variables $x(t) = [c_s^+(r,t), c_s^-(r,t), c_e^+(x,t), c_e^{sep}(x,t), c_e^-(x,t), T(t)]^T$. The constraints include the model dynamics and boundary conditions (1) - (9), input, state, event, and time constraints below:

$$
\begin{aligned}
I_{min} \le I(t) \le I_{max}, &\qquad (16)\\
\theta_{min}^{\pm} \le \frac{c_s^{\pm}(r,t)}{c_{s,max}} \le \theta_{max}^{\pm}, &\qquad (17)\\
c_{e,min} \le c_e^l(x,t) \le c_{e,max}, \quad l \in \{-,\text{sep},+\} &\qquad (18)\\
T_{min} \le T(t) \le T_{max}, &\qquad (19)\\
t_0 \le t_f \le t_{max}, &\qquad (20)\\
c_s^{\pm}(r,t_0) = c_{s,0}^{\pm}, \quad c_e^l(x,t_0) = c_{e,0}^l, \quad l \in \{-,\text{sep},+\} &\qquad (21)\\
T(t_0) = T_0, \qquad SOC(t_0) = SOC_0, &\qquad (22)\\
SOC(t_f) = SOC_f. &\qquad (23)
\end{aligned}
$$

Constraints (17) - (18) protect the solid active material and electrolyte from lithium depletion/oversaturation. Constraint (19) protects against excessively cold or hot temperatures that accelerate cell aging.

The PDE system (1)-(9) is discretized in space using a second-order accurate finite central difference method that conserves lithium [28], resulting in a nonlinear differential algebraic equation system. Due to this complex mathematical structure, it is difficult to use conventional optimization techniques, e.g., dynamic programming, Pontryagin's minimum principle, and indirect methods, due to intractable computational burden or accuracy. Instead, we pursue pseudo-spectral methods to transcribe this infinite-dimensional optimal control problem into a finite-dimensional optimization problem with algebraic constraints at the discretized nodes. Then, the optimization variables at such nodes are solved by off-the-shelf nonlinear programming (NLP) solvers, like SNOPT or IPOPT [29]. Note that convexity is not guaranteed, and therefore these solvers yield locally optimal solutions. Pseudo-spectral methods are an effective tool for complex nonlinear optimal control problems and have been extensively applied to real-world optimization problems in engineering, including aerospace and autonomous flight systems [30], road vehicle systems [31], energy storage [20], [21], etc. There are a myriad of approaches for discretizing integral and differential equations, leading to a spectrum of pseudo-spectral variants. In this study, we use the Legendre-Gauss-Radau (LGR) pseudo-spectral method with adaptive multi-mesh-interval collocation, featured by the general purpose optimal control software (GPOPS-II) [29]. This software incorporates an orthogonal collocation method to generate the LGR points. Rather than a traditional fixed global mesh, an adaptive mesh refinement algorithm is employed to iteratively adjust the number of mesh intervals, the width of each interval, and the polynomial degree (the number of LGR points). Theoretical and algorithmic properties of this method are elaborated in [32], [33].

IV. Results and Discussion

This section presents optimization results for minimum-time charge and examines solution sensitivity to perturba-

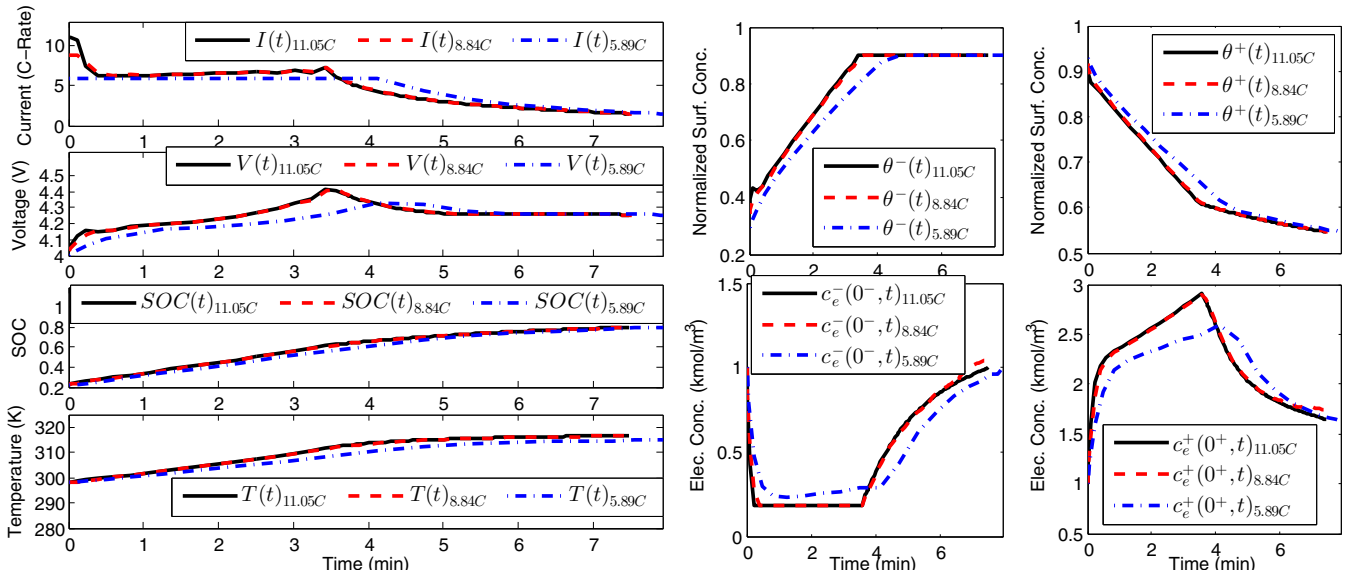

Fig. 3. Optimization results for minimum time charge with $I_{max} = \{11.05C, 8.84C, 5.89C\}$. Left: Current $I(t)$, Voltage $V(t)$, State of Charge $SOC(t)$, Temperature $T(t)$. Right: Surface Concentrations $\theta^-(t), \theta^+(t)$, Electrolyte Concentrations $c_e^-(0^-,t), c_e^+(0^+,t)$.

tions in model parameters.

A. Minimum Time Charge

The optimal charge trajectories are shown in Fig. 3 for $I_{max} = \{11.05C, 8.84C, 5.89C\}$. It takes 7.4721min to achieve a target SOC of 80% ($SOC_f = 0.8$) from an initial SOC of 20% ($SOC_0 = 0.2$) when $I_{max} = 11.05C$. The charge process follows a constant-current/constant-electrolyte-concentration/constant-surface-concentration (CC-CCe-CCss) protocol. To minimize charging time, the maximum C-rate is applied initially, causing the minimum electrolyte concentration constraint to become active at the anode current collector. The surface concentration at the anode increases until it reaches its maximum value, which becomes the dominant inequality constraint. A similar behavior is observed when $I_{max} = 8.84C$, with a longer initial current at the maximum C-rate. It takes 7.5099min to achieve the target SOC in this case, which is slightly more than the previous case. Note that once the the minimum electrolyte concentration constraint becomes active at the anode current collector, the protocol follows almost the same trajectory as the previous case. A slightly different behavior is observed when $I_{max} = 5.89C$, which just has 2 steps. It takes 7.9238min to achieve the target SOC in this case, which is longer in time than the previous cases. This protocol follows a constant-current/constant-surface-concentration (CC-CCss) protocol. The maximum C-rate is applied initially, until the maximum surface concentration at the anode constraint becomes active. Heuristically, the first two protocols where $I_{max} = \{11.05C, 8.84C\}$ are similar in nature to the CC-CC-CV charge protocol [5] which involves an initial high constant current period, followed by a lower constant current period, and then by a constant voltage period. The last protocol where $I_{max} = 5.89C$ is similar in nature to the well known CC-CV protocol [4].

A comparison of the optimized charge protocol vs. the well known CC-CV protocol is presented in Fig. 4 for $I_{max} = 5.89C$. We make two observations. (i) It takes the CC-CV protocol 9.0041min to achieve the target SOC, a 1.0803min (13.63%) increase w.r.t. the optimized charge protocol at $I_{max} = 5.89C$. (ii) The optimized protocol allows safe excursions beyond the 4.2V upper limit in CC-CV by ensuring the electrochemical state constraints are satisfied.

B. Sensitivity Based Battery Design for Fast Charging

Next we examine the solution sensitivity to perturbations in model parameters for fast charging. In previous results, we noted that the first electrochemical constraint to become active was the electrolyte concentration at the anode current collector when $I_{max} = \{11.05C, 8.84C\}$. This observation motivates exploring how alterations to the electrolyte dynamics impact minimum charge time.

1) Electrolyte Diffusivity $D_e(c_e)$: A comparison between the optimized charge protocol for a $\pm 5\%$ deviation in $D_e(c_e)$ and the solution with nominal parameters is shown in Fig. 5 for $I_{max} = 8.84C$. The optimized charge protocol with a $+5\%$ deviation requires 7.3866min to achieve the target SOC. The cell with greater electrolyte diffusivity requires 0.1234min (1.64%) less charge time. Consequently, increasing $D_e(c_e)$ is favorable to obtaining a faster charge time. The optimized charge protocol with a -5% deviation requires 7.6463min to achieve the target SOC. The cell with lower electrolyte diffusivity requires 0.1363min (1.82%) more charge time. Consequently, decreasing $D_e(c_e)$ is not favorable to obtaining a faster charge time. Note that the trajectories are similar to that of the unperturbed solution. The difference is seen in the electrolyte concentration dynamics which become faster or slower depending on the increase or decrease in $D_e(c_e)$, respectively.

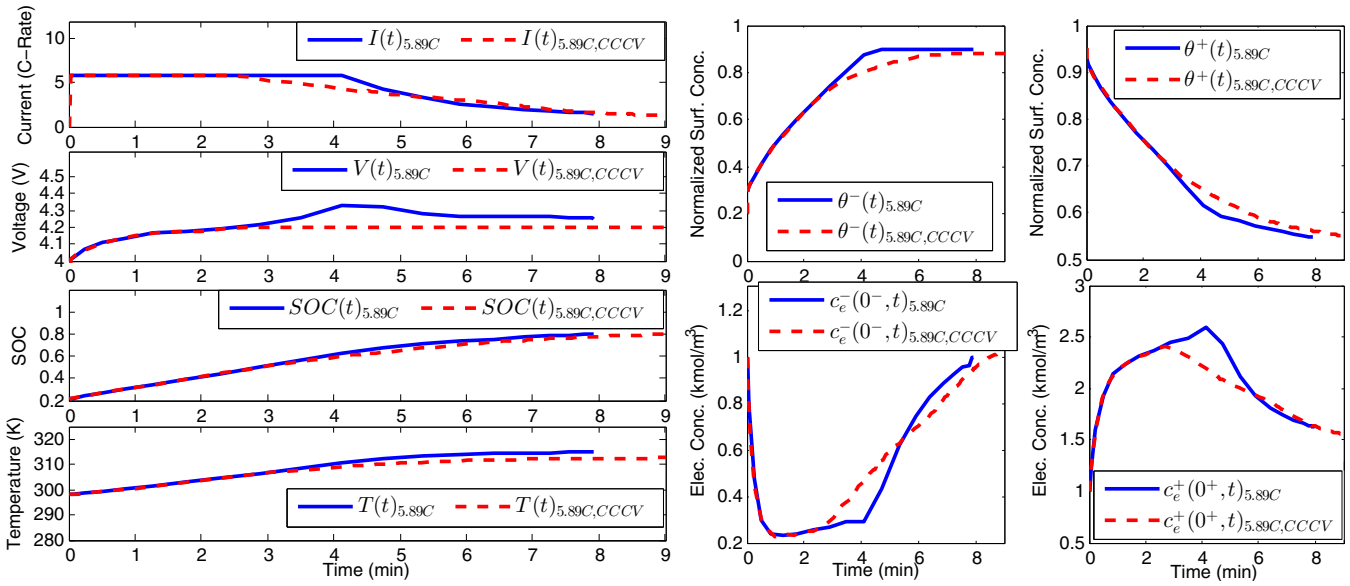

Fig. 4. Optimized charge vs. CC-CV charge trajectories with $I_{max} = 5.89C$. Left: Current $I(t)$, Voltage $V(t)$, State of Charge $SOC(t)$, Temperature $T(t)$. Right: Surface Concentrations $\theta^-(t), \theta^+(t)$, Electrolyte Concentrations $c_e^-(0^-,t), c_e^+(0^+,t)$.

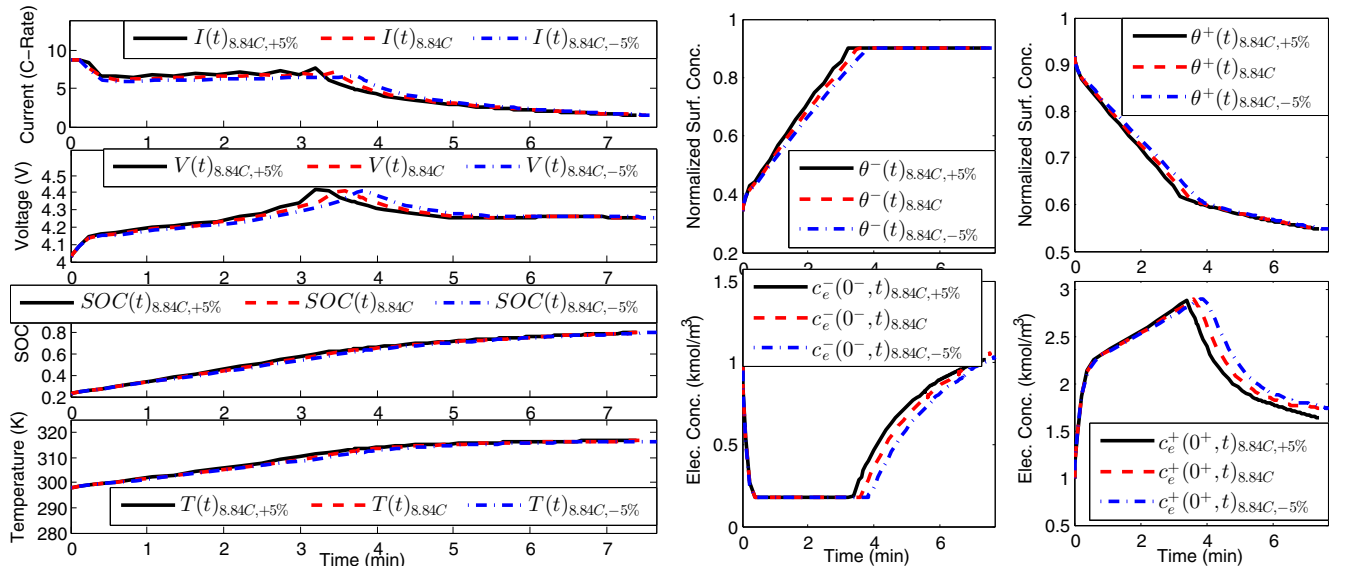

Fig. 5. Influence of a $\pm 5\%$ deviation in $D_e(c_e)$ on optimization results for minimum time charge with $I_{max} = 8.84C$. Left: Current $I(t)$, Voltage $V(t)$, State of Charge $SOC(t)$, Temperature $T(t)$. Right: Surface Concentrations $\theta^-(t), \theta^+(t)$, Electrolyte Concentrations $c_e^-(0^-,t), c_e^+(0^+,t)$.

V. Conclusions

An optimal control framework for a PDE system has been developed to explore model-based fast-safe charging protocols. In this framework, a coupled Single Particle Model with Electrolyte and Thermal Dynamics is incorporated to account for solid and electrolyte phase concentration constraints, as well as thermal constraints. The Legendre-Gauss-Radau (LGR) pseudo-spectral method with adaptive multi-mesh-interval collocation is leveraged to solve the infinite dimensional nonlinear optimal control problem.

Charge time is examined subject to both electrochemical and thermal constraints. The resulting minimum time charge regimes with varying input current limits are analyzed in detail, with the following key findings: (i) The protocol is constant-current/constant-electrolyte-concentration/constant-surface-concentration (CC-CCe-CCss) when $I_{max} = \{11.05C, 8.84C\}$, requiring 7.4721 minutes and 7.5099 minutes to charge the battery from 20% to 80% SOC, respectively. This optimized protocol is similar to the heuristic high constant current-low constant current-constant voltage (CC-CC-CV) protocol. (ii) The protocol is constant-current/constant-surface-concentration (CC-CCss) when $I_{max} = 5.89C$, requiring 7.9238 minutes to charge the battery and is similar to the well known

constant-current/constant-voltage (CC-CV) protocol. (iii) The protocol solutions yield physical insight on which battery design parameters to optimize for fast charging applications. Increasing electrolyte diffusivity coefficient $D_e(c_e)$ results in faster charge time when $I_{max} = 8.84C$.

In this paper we assume full state measurements and known parameters to ascertain the maximum possible fast charging benefits of SPMeT-based control. Future work combines the SPMeT presented here with state and parameter estimates generated by adaptive PDE observers [1]. This output feedback system (i) guards against harmful operating regimes, (ii) increases charging speed, and (iii) monitors state-of-charge and state-of-health, all from measurements of voltage, current, and temperature. Future work also include incorporation of progressive aging dynamics, similar to [21]. Finally, we plan to experimentally quantify the aforementioned benefits on a battery-in-the-loop test facility.

REFERENCES

[1] S. J. Moura, N. Chaturvedi, and M. Krstic, "Adaptive PDE Observer for Battery SOC/SOH Estimation via an Electrochemical Model," *ASME Journal of Dynamic Systems, Measurement, and Control*, vol. 136, no. 1, pp. 011 015–011 026, Oct 2014.

[2] X. Hu, N. Murgovski, L. Johannesson, and B. Egardt, "Comparison of Three Electrochemical Energy Buffers Applied to a Hybrid Bus Powertrain With Simultaneous Optimal Sizing and Energy Management," *IEEE Transactions on Intelligent Transportation Systems*, vol. 15, no. 3, pp. 1193–1205, June 2014.

[3] M. Yilmaz and P. Krein, "Review of Battery Charger Topologies, Charging Power Levels, and Infrastructure for Plug-In Electric and Hybrid Vehicles," *IEEE Transactions on Power Electronics*, vol. 28, no. 5, pp. 2151–2169, May 2013.

[4] S. Zhang, K. Xu, and T. Jow, "Study of the charging process of a LiCoO2-based Li-ion battery," *Journal of Power Sources*, vol. 160, no. 2, pp. 1349 – 1354, 2006.

[5] D. Ansean, M. Gonzalez, J. Viera, V. Garcia, C. Blanco, and M. Valledor, "Fast charging technique for high power lithium iron phosphate batteries: A cycle life analysis," *Journal of Power Sources*, vol. 239, no. 0, pp. 9 – 15, 2013.

[6] P. Notten, J. O. het Veld, and J. van Beek, "Boostcharging Li-ion batteries: A challenging new charging concept," *Journal of Power Sources*, vol. 145, no. 1, pp. 89 – 94, 2005.

[7] S. S. Zhang, "The effect of the charging protocol on the cycle life of a Li-ion battery," *Journal of Power Sources*, vol. 161, no. 2, pp. 1385 – 1391, 2006.

[8] H. Surmann, "Genetic optimization of a fuzzy system for charging batteries," *IEEE Transactions on Industrial Electronics*, vol. 43, no. 5, pp. 541–548, Oct 1996.

[9] Y.-H. Liu and Y.-F. Luo, "Search for an optimal rapid-charging pattern for li-ion batteries using the taguchi approach," *IEEE Transactions on Industrial Electronics*, vol. 57, no. 12, pp. 3963–3971, Dec 2010.

[10] Z. Ullah, B. Burford, and S. Dillip, "Fast intelligent battery charging: neural-fuzzy approach," *IEEE Aerospace and Electronic Systems Magazine*, vol. 11, no. 6, pp. 26–34, Jun 1996.

[11] L.-R. Chen, R. Hsu, and C.-S. Liu, "A design of a grey-predicted li-ion battery charge system," *IEEE Transactions on Industrial Electronics*, vol. 55, no. 10, pp. 3692–3701, Oct 2008.

[12] Y.-H. Liu, J.-H. Teng, and Y.-C. Lin, "Search for an optimal rapid charging pattern for lithium-ion batteries using ant colony system algorithm," *IEEE Transactions on Industrial Electronics*, vol. 52, no. 5, pp. 1328–1336, Oct 2005.

[13] M. A. Monem, K. Trad, N. Omar, O. Hegazy, B. Mantels, G. Mulder, P. V. den Bossche, and J. V. Mierlo, "Lithium-ion batteries: Evaluation study of different charging methodologies based on aging process," *Applied Energy*, vol. 152, no. 0, pp. 143 – 155, 2015.

[14] Y. Parvini and A. Vahidi, "Maximizing Charging Efficiency of Lithium-Ion and Lead-Acid Batteries Using Optimal Control Theory," in *2015 American Control Conference*, Chicago, IL USA, July 1-3 2015.

[15] A. Abdollahi, N. Raghunathan, X. Han, G. V. Avvari, B. Balasingam, K. R. Pattipati, and Y. Bar-Shalom, "Battery Charging Optimization for OCV-Resistance Equivalent Circuit Model," in *2015 American Control Conference*, Chicago, IL USA, 2015.

[16] R. Methekar, V. Ramadesigan, R. D. Braatz, and V. R. Subramanian, "Optimum charging profile for lithium-ion batteries to maximize energy storage and utilization," *ECS Transactions*, vol. 25, no. 35, pp. 139–146, 2010.

[17] M. Torchio, N. A. Wolff, D. M. Raimondo, L. Magni, U. Krewer, R. B. Gopaluni, J. A. Paulson, and R. D. Braatz, "Real-time Model Predictive Control for the Optimal Charging of a Lithium-ion Battery," in *2015 American Control Conference*, Chicago, IL USA, 2015.

[18] R. Klein, N. Chaturvedi, J. Christensen, J. Ahmed, R. Findeisen, and A. Kojic, "Optimal charging strategies in lithium-ion battery," in *American Control Conference (ACC), 2011*, June 2011, pp. 382–387.

[19] H. Perez, N. Shahmohammadhamedani, and S. Moura, "Enhanced performance of li-ion batteries via modified reference governors and electrochemical models," *IEEE/ASME Transactions on Mechatronics*, vol. 20, no. 4, pp. 1511–1520, Aug 2015.

[20] X. Hu, S. Li, H. Peng, and F. Sun, "Charging time and loss optimization for LiNMC and LiFePO4 batteries based on equivalent circuit models," *Journal of Power Sources*, vol. 239, no. 0, pp. 449 – 457, 2013.

[21] X. Hu, H. E. Perez, and S. J. Moura, "Battery charge control with an electro-thermal-aging coupling," in *ASME 2015 Dynamic Systems and Control Conference*, Dynamic Systems and Control Division. Columbus, Ohio, USA: ASME, October 2015.

[22] E. Prada, D. D. Domenico, a. J. B. Y. Creff, V. Sauvant-Moynot, and F. Huet, "Simplified electrochemical and thermal model of LiFePO4-graphite li-ion batteries for fast charge applications," *Journal of The Electrochemical Society*, vol. 159, no. 9, pp. A1508–A1519, 2012.

[23] P. Kemper and D. Kum, "Extended Single Particle Model of Li-Ion Batteries Towards High Current Applications," in *2013 IEEE Vehicle Power and Propulsion Conference (VPPC)*, Oct 2013, pp. 1–6.

[24] X. Han, M. Ouyang, L. Lu, and J. Li, "Simplification of physics-based electrochemical model for lithium ion battery on electric vehicle. Part I: Diffusion simplification and single particle model," *Journal of Power Sources*, vol. 278, pp. 802 – 813, 2015.

[25] S. J. Moura, F. B. Argomedo, R. Klein, A. Mirtabatabaei, and M. Krstic. (2015) Battery state estimation for a single particle model with electrolyte dynamics. UC Berkeley: Energy, Controls, and Applications Lab. [Online]. Available: http://escholarship.org/uc/item/5xt11817

[26] D. Bernardi, E. Pawlikowski, and J. Newman, "A general energy balance for battery systems," *Journal of the Electrochemical Society*, vol. 132, no. 1, pp. 5–12, 1985.

[27] J. Newman. (2008) Fortran programs for the simulation of electrochemical systems. [Online]. Available: http://www.cchem.berkeley.edu/jsngrp/fortran.html

[28] J. Strikwerda, *Finite difference schemes and partial differential equations*. Society for Industrial and Applied Mathematics, 2007.

[29] M. A. Patterson and A. V. Rao, "GPOPS-II: A MATLAB software for solving multiple-phase optimal control problems using hp-adaptive gaussian quadrature collocation methods and sparse nonlinear programming," *ACM Trans. on Mathematical Software (TOMS)*, vol. 41, no. 1, 2014.

[30] I. M. Ross and M. Karpenko, "A review of pseudospectral optimal control: From theory to flight," *Annual Reviews in Control*, vol. 36, no. 2, pp. 182 – 197, 2012.

[31] D. Limebeer, G. Perantoni, and A. Rao, "Optimal control of formula one car energy recovery systems," *International Journal of Control*, vol. 87, no. 10, pp. 2065–2080, 2014.

[32] C. L. Darby, W. W. Hager, and A. V. Rao, "An hp-adaptive pseudospectral method for solving optimal control problems," *Optimal Control Applications and Methods*, vol. 32, no. 4, pp. 476–502, 2011.

[33] D. Garg, W. W. Hager, and A. V. Rao, "Pseudospectral methods for solving infinite-horizon optimal control problems," *Automatica*, vol. 47, no. 4, pp. 829 – 837, 2011.